Reexamining linkages between US east coast sea level and the AMOC

Christopher Little (clittle@aer.com) (Atmospheric and Environmental Research, Inc)

Aixue Hu, Chris W. Hughes, Gerard McCarthy, Christopher G. Piecuch, Rui M. Ponte, Matthew D. Thomas

Motivation

United States east coast (USEC) sea level rise is already having adverse environmental, societal, and economic consequences. Looking forward through the 21st century, regional ocean dynamics related to the Atlantic Meridional Overturning Circulation (AMOC) have the potential to drive disproportionately high rates of coastal sea level rise along the US east coast relative to other locations (i.e. "sea level rise hotspots").

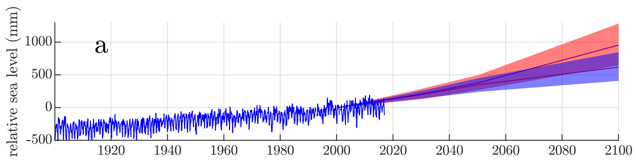

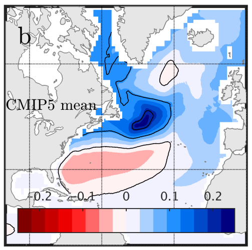

a) Monthly mean tide gauge sea level (in mm relative to year 2000) at the Battery (New York City) (blue line). Projections of ***relative sea level*** *(RSL) change, relative to year 2000, for RCP 2.6 (blue) and RCP 8.5 emissions scenarios (red) (Kopp et al., 2014). Shading indicates 17-83rd percentile range of RSL projections. b) CMIP5 RCP 4.5 ensemble mean* ***dynamic sea level*** *(DSL) change from 1976-2000 to 2076-2100 (in m).*

Over the past decade, scientific and societal interest in the relationship between AMOC and USEC sea level have been addressed by a wealth of research studies, both model- and observationally-based. This poster highlights some of the conclusions of a recently-submitted review paper.

Theoretical basis for an AMOC-sea level relationship

$$\rho_0 \frac{h_W}{Q} = -\frac{f}{gH_e}$$

Predictions:

- **Scaling coefficient between 1-2 cmSv^{-1}**
- **Weak along-coast gradients**

Assumptions:

- **Applies only to zonally integrated transport (Q)**
- **Temporally constant vertical velocity profile (He)**
- **Negligible ageostropic and nonlinear terms**

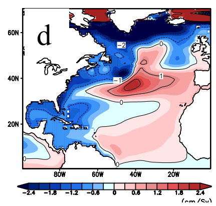

Regression coefficient of annual mean sea level and AMOC transport (at the same latitude) between 100 and 1300 m using a 1° ocean model, for the period 1950–2009, without wind forcing (from Woodworth et al., 2014).

A diagnostic relationship between the AMOC and DSL can be derived from the zonal momentum equation:

$$\frac{\rho}{r\cos\phi}\frac{D}{Dt}(ur\cos\phi) - \rho f v + \rho f w \cot\phi = -\frac{1}{r\cos\phi}\frac{\partial p}{\partial\lambda} + F_x, \quad (1)$$

where u is the zonal velocity and w the vertical velocity, f is the Coriolis frequency, ϕ is latitude, λ is longitude, p is pressure, ρ is density, F_x is the eastward viscous force per unit volume, and D/Dt is the material rate of change.

If we: 1) zonally integrate over the basin; and 2) neglect the advection of relative angular momentum (the first term), the term involving w (usually neglected in the Primitive Equations), and the viscous term, this reduces to an integrated geostrophic balance:

$$fT = p_E - p_W, \quad (2)$$

Equation (2) relates the meridional northward mass transport at each latitude (T; the zonal integral of ρv) to bottom pressure at the eastern (p_E) and the western boundary (p_W).

First, we note that the eastern boundary pressure is very close to being a function of depth alone, independent of latitude, at least below a depth of around 100 m (Hughes & de Cuevas, 2001). Subtracting off this reference function of depth in our definition of p (which now should be considered to be a pressure anomaly, referenced to the eastern boundary value), we find that $p_E = 0$. Then, integrating over depth from the surface ($z = 0$) to the depth of the maximum in the overturning streamfunction ($z = -H$), we find that the total northward mass transport above this depth is given by

$$Q = \int_{-H}^{0} T\,dz = -\frac{1}{f}\int_{-H}^{0} p_W\,dz = -\frac{H}{f}\overline{p_W}, \quad (3)$$

where $\overline{p_W}$ is the western boundary pressure averaged over the depth range above the maximum overturning. The relationship to coastal sea level then follows from the assumption that the depth averaged pressure in this zone is related to the boundary pressure near the surface, p_{W0}, which is in turn related to inverse barometer-corrected boundary sea level h_W by $\rho_0 g h_W = p_{W0}$, where we use a reference density ρ_0. Rewriting in terms of this near-surface western boundary pressure anomaly, we find

$$Q = -\frac{H_e}{f}p_{W0} = -\frac{H_e}{f}\rho_0 g h_W, \quad (4)$$

which requires the definition of an effective layer thickness

$$H_e = \int_{-H}^{0}\frac{p_W}{p_{W0}}dz, \quad (5)$$

which would be equal to H if the pressure anomaly (or equivalently the northward transport) was independent of depth above $z = -H$. If the zonally-integrated flow (or pressure anomaly) was largest at the surface and decreased linearly to zero at the maximum of the overturning, we would have $H_e = 0.5H$. Rearranging, we find that the coastal sea-level signal can be written as

$$h_W = -\frac{Q}{\rho_0}\frac{f}{gH_e}, \quad (6)$$

in which it is shown how the coastal sea-level signal h_W is negatively related to the strength of the overturning Q/ρ_0, and the size of the signal is larger if the effective layer thickness H_e is smaller. With uniform northward zonally-integrated flow above about 1000 m depth, equation (6) predicts a sea-level change of 1 cm per Sverdrup of meridional transport. With a linear increase in velocity from zero at 1000 m to a maximum at the surface, then pressure at the surface is twice the depth-average, leading to a scaling of -2 cm Sv^{-1}.

The AMOC-sea level relationship in CMIP5 RCP 4.5 simulations

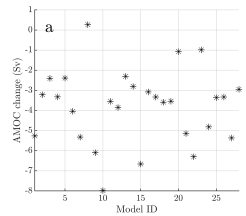

$$\Delta\,\mathrm{DSL}\,(x,y,m) = \alpha(x,y)\Delta\mathrm{AMOC}\,(m) + \varepsilon(x,y,m)$$

a) Change in maximum AMOC strength for a 28 CMIP5 model, RCP4.5-forced, ensemble, from 1976-2000 to 2076-2100, as calculated by Chen et al. (2018). c) Linear regression coefficient (α) of DSL change against the change in maximum AMOC strength for the models shown in (a) (m/Sv). e) Variance in DSL change explained by AMOC change (%).

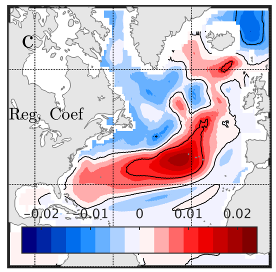

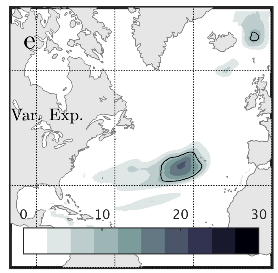

$$\Delta\,\mathrm{DSL}\,(x,y,m)/\Delta\mathrm{AMOC}\,(m)$$

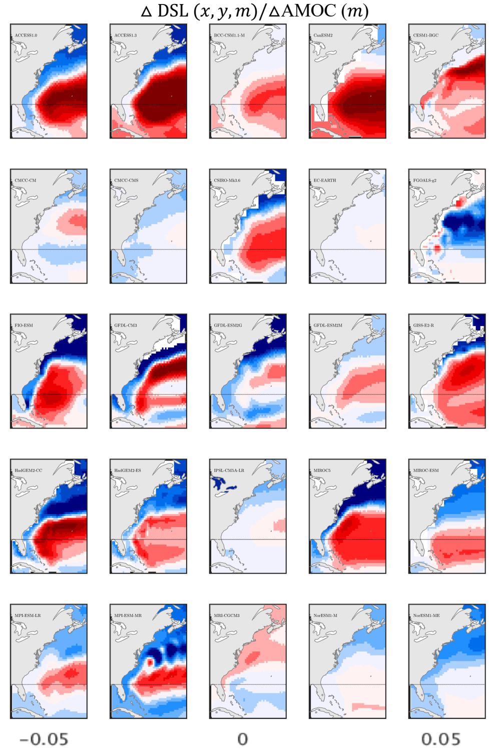

Map of the ratio of DSL change to AMOC change (in m/Sv; 2076-2100 minus 1976-2000) for 25 RCP4.5-forced CMIP5 models with AMOC weakening larger than 2 Sv.

Conclusions

- **Numerical models and theoretical considerations support an anti-phase relationship between AMOC strength and dynamic sea level along the US east coast.**
- **However, the amplitude and pattern of sea-level variability associated with AMOC variations is forcing-, timescale-, location-, and model-dependent**
- **Observational analyses focusing on shorter (generally less than decadal) timescales show robust relationships between some components of the North Atlantic large-scale circulation and coastal sea-level variability, but the causal relationships between different observational metrics, AMOC, and sea level are often unclear.**

Ways forward

New research, and the incorporation of existing research, that seeks to understand:

- **Relationships between AMOC and its component currents**
- **The role of ageostrophic processes near the coast**
- **The interplay of local (continental-shelf) and remote forcing**
- **Causal drivers of AMOC changes (e.g. wind vs. buoyancy forcing)**

Observations

- **OSNAP array: perspective on AMOC's meridional coherence (Lozier et al. 2017)**
- **New campaigns over the USEC shelf and slope (Gawarkiewicz et al. 2018)**

Models

- **Broadening metrics of ocean circulation beyond the maximum AMOC strength**
- **High-resolution simulations**
- **Assessment of momentum budgets**

The AMOC-sea level relationship in observations

Direct AMOC monitoring only available since 2004

- **Goddard et al. (2015) find a relationship with interannual AMOC anomalies.**
- **Piecuch et al. 2015 and Piecuch et al. 2016 show this is largely due to local atmospheric forcing; Piecuch et al. (in review) show that correlation arises from LOCAL ageostrophic responses of northeast US sea level and Ekman transport across 26°N by large-scale wind field.**

Indirect evidence (AMOC "proxies")

- **Florida current/Gulf Stream strength (e.g. Park and Sweet 2013; Ezer 2013)**
- **Gulf Stream North Wall (e.g. Kopp et al. 2013, McCarthy et al. 2015)**
- **SPG heat content and density differences (McCarthy et al. 2015; Frederikse et al. 2017)**

- **All indirect evidence relies on a (generally model-derived) relationship between AMOC proxies and AMOC strength**

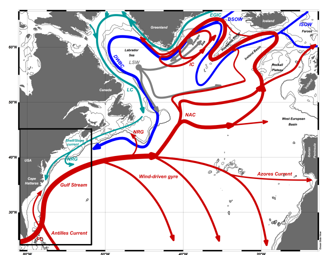

Schematic of key AMOC-related components of the North Atlantic Ocean (modified from García-Ibáñez et al., 2018). Abbreviations are as follows: FC=Florida Current; NRG=Northern Recirculation Gyre, LC=Labrador Current; NAC=North Atlantic Current; DWBC=Deep Western Boundary Current; IC=Irminger Current; EGIC= East Greenland Current. Three source waters for NADW are noted: LSW=Labrador Sea Water; ISOW=Iceland-Scotland Overflow Water; DSOW= Denmark Straits Overflow Water. Box indicates the USEC region.

References

Chen, C., Liu, W., & Wang, G. (2018). Understanding the uncertainty in the 21st century dynamic sea level projections: the role of the AMOC. *Geophysical Research Letters*.

Ezer, T., Atkinson, L. P., Corlett, W. B., & Blanco, J. L. (2013). Gulf Stream's induced sea level rise and variability along the U.S. mid-Atlantic coast. *Journal of Geophysical Research: Oceans*, *118*(2), 685–697.

Frederikse, T., Simon, K., Katsman, C. A., & Riva, R. (2017). The sea-level budget along the Northwest Atlantic coast: GIA, mass changes, and large-scale ocean dynamics. *Journal of Geophysical Research: Oceans*, *122*(7), 5486–5501.

Gawarkiewicz, G., R.E. Todd, W. Zhang, J. Partida, A. Gangopadhyay, M.-U.-H. Monim, P. Fratantoni, A. Malek Mercer, and M. Dent. 2018. The changing nature of shelf-break exchange revealed by the OOI Pioneer Array. *Oceanography* 31(1):60–70.

Goddard, P. B., Yin, J., Griffies, S. M., & Zhang, S. (2015). An extreme event of sea-level rise along the Northeast coast of North America in 2009–2010. *Nature Communications*, *6*(1).

Hughes, C. W., & de Cuevas, B. A. (2001). Why Western Boundary Currents in Realistic Oceans are Inviscid: A Link between Form Stress and Bottom Pressure Torques. *Journal of Physical Oceanography*, *31*(10), 2871–2885.

Kopp, R. E. (2013). Does the mid-Atlantic United States sea level acceleration hot spot reflect ocean dynamic variability?. *Geophysical Research Letters*, *40*(15), 3981–3985.

Kopp, R. E., Horton, R. M., Little, C. M., Mitrovica, J. X., Oppenheimer, M., Rasmussen, D. J., et al. (2014). Probabilistic 21st and 22nd century sea-level projections at a global network of tide-gauge sites. *Earth's Future*, *2*(8), 383–406.

Lozier, M. S., Bacon, S., Bower, A. S., Cunningham, S. A., Femke de Jong, M., de Steur, L., et al. (2017). Overturning in the Subpolar North Atlantic Program: A New International Ocean Observing System. *Bulletin of the American Meteorological Society*, 98(4), 737–752.

McCarthy, G. D., Haigh, I. D., Hirschi, J. J.-M., Grist, J. P., & Smeed, D. A. (2015). Ocean impact on decadal Atlantic climate variability revealed by sea-level observations. *Nature*, *521*(7553), 508–510.

Park, J., & Sweet, W. (2015). Accelerated sea level rise and Florida Current transport. *Ocean Science*, *11*(4), 607–615. https://doi.org/10.5194/os-11-607-2015

Piecuch, C. G., & Ponte, R. M. (2015). Inverted barometer contributions to recent sea level changes along the northeast coast of North America. *Geophysical Research Letters*, *42*(14), 5918–5925.

Piecuch, C. G., Dangendorf, S., Ponte, R. M., & Marcos, M. (2016). Annual sea level changes on the North American Northeast Coast: influence of local winds and barotropic motions. *Journal of Climate*, *29*(13), 4801–4816.

Woodworth, Philip L., Maqueda, M. Á. M., Roussenov, V. M., Williams, R. G., & Hughes, C. W. (2014). Mean sea-level variability along the northeast American Atlantic coast and the roles of the wind and the overturning circulation. Journal of Geophysical Research: Oceans, 119(12), 8916–8935.

Acknowledgements

- **Support from NSF grant OCE-1805029 (CML) and NASA contract NNH16CT01C (CML, RMP), the U.S. Department of Energy's Office of Biological & Environmental Research Cooperative Agreement # DE-FC02-97ER62402 (AH), Natural Environment Research Council NE/K012789/1 (CWH), Irish Marine Institute Project A4 PBA/CC/18/01 (GDM), NSF awards OCE-1558966 and OCE-1834739 (CGP).**
- **The NOAA Geophysical Fluid Dynamics Laboratory, for computational and analysis tools.**
- **CLIVAR and the US AMOC Science Team for inspiration and patience as the manuscript evolved.**